

Nanoscale

Accepted Manuscript



This is an *Accepted Manuscript*, which has been through the Royal Society of Chemistry peer review process and has been accepted for publication.

Accepted Manuscripts are published online shortly after acceptance, before technical editing, formatting and proof reading. Using this free service, authors can make their results available to the community, in citable form, before we publish the edited article. We will replace this *Accepted Manuscript* with the edited and formatted *Advance Article* as soon as it is available.

You can find more information about *Accepted Manuscripts* in the [Information for Authors](#).

Please note that technical editing may introduce minor changes to the text and/or graphics, which may alter content. The journal's standard [Terms & Conditions](#) and the [Ethical guidelines](#) still apply. In no event shall the Royal Society of Chemistry be held responsible for any errors or omissions in this *Accepted Manuscript* or any consequences arising from the use of any information it contains.

Clathrin-mediated internalization of micelles based on chondroitin sulfate-graft-poly(ϵ -caprolactone) causing distinct CPT-induced deaths in lung cancer

Yu-Sheng Liu^{#1,2}, Ru-You Cheng^{#2}, Yu-Lun Lo², Chin Hsu³, Su-Hwei Chen¹, Chien-Chih Chiu^{4*}, and
Li-Fang Wang^{2,5*}

¹*School of Pharmacy, Kaohsiung Medical University, Kaohsiung 807, Taiwan*

²*Department of Medicinal and Applied Chemistry, College of Life Science, Kaohsiung Medical University, Kaohsiung 807, Taiwan*

³*Department of Physiology, Faculty of Medicine, College of Medicine, Kaohsiung Medical University, Kaohsiung 80708, Taiwan*

⁴*Department of Biotechnology, College of Life Science, Kaohsiung Medical University, Kaohsiung 80708, Taiwan*

⁵*Institute of Medical Science and Technology, National Sun Yat-Sen University, Kaohsiung 804, Taiwan*

***Corresponding authors**

#Equal contribution

Correspondence to Li-Fang Wang, Professor of Medicinal & Applied Chemistry

Kaohsiung Medical University
School of Life Science
100, Shih-Chuan 1st Rd, Kaohsiung City 807, Taiwan
Tel: 011-886-7-3121101-2217
Fax: 011-886-7-3125339
E-mail: lfwang@kmu.edu.tw

Manuscript submitted to *Nanoscale* on November 25, 2015.

Revised on December 28, 2015

Abstract

Our previous research has synthesized a chondroitin sulfate-*graft*-poly(ϵ -caprolactone) copolymer with a high content of poly(ϵ -caprolactone) (18.7 mol%), named H-CP, which self-assembled in water into a rod-like micelle to encapsulate the hydrophobic camptothecin in the core (micelle/CPT) for tumor-targeting delivery. Owing to recognition of the micelle to CD44, the micelle/CPT entered CRL-5802 cells efficiently and released CPT efficaciously, thus showing higher tumor suppression than a commercial product, CPT-11. In this study, H1299 cells were found to have higher CD44 expression than CRL-5802 cells. However, the lower CD44-expressing CRL-5802 cells had higher cell death and higher cellular uptake of the micelle/CPT compared with the higher CD44-expressing H1299 cells. Examining the internalization pathway of the micelle/CPT in the presence of different endocytic chemical inhibitors showed that CRL-5802 cells involved clathrin-mediated endocytosis which was not found in H1299 cells. Analysis on the cell cycle of the two cell lines exposed to the micelle/CPT revealed that CRL-5802 cells arrested mainly in the S phase and H1299 cells, mainly in the G2-M phase. A consistent result was also found in the evaluation of γ -H2AX expression, showing around three-fold higher in CRL-5802 cells than in H1299 cells. A near-IR dye, IR780 was encapsulated into the micelle to observe the *in vivo* biodistribution of micelle/IR780 in tumor-bearing mice. The CRL-5802 tumor indeed showed higher fluorescence intensity than the H1299 tumor at any tracing time points following 1 hour. Thus, we tentatively conclude CRL-5802 utilized the clathrin-mediated

internalization pathway and arrested in the S phase upon exposure to the micelle/CPT; all are possible reasons for better therapeutic outcome in CRL-5802 cells than in H1299 cells.

Introduction

Chondroitin sulfate (CS) is a natural polysaccharide, having many merits such as biocompatibility, biodegradability,¹ serving as an anti-inflammatory agent,² and a natural ligand for the cluster determinant (CD44) receptor.³ The CD44 receptor is one of the membrane receptors overexpressing on many solid tumor surfaces.^{4,5} Thus, CS can be used as a specific molecular ligand for targeting cancer cells through CD44-mediated endocytosis.³

A copolymer based on CS and polycaprolactone (PCL), named CP, was synthesized as an anticancer drug carrier.⁶ Both CS and PCL are FDA-approved nontoxic materials. Owing to amphiphilicity, the CP copolymer could self-assemble into micelles in water, which could be utilized to encapsulate a hydrophobic anticancer drug, camptothecin (CPT), in the core for tumor-targeting delivery. CPT is an antineoplastic agent and has a low aqueous solubility and short-term stability of the lactone ring structure, thus limiting its development in clinical settings.^{7,8} The advantages of using the CP self-assembled micelles in drug delivery include not only recognition to CD44 but also saving the lactone ring of CPT in blood circulation. Moreover, a polysaccharide-modified nanoparticle prevents recognition by the reticuloendothelial system (RES),^{9,10} similar to the role of poly(ethylene glycol).

The physicochemical properties of the micelle and CPT-loaded micelle (micelle/CPT) were thoroughly characterized and the therapeutic efficacy of the micelle/CPT was demonstrated in non-small cell lung cancer (NSCLC) CRL-5802 cells, expressing the CD44 receptor on cell surface.⁶ The CD44-expressing intensity on the surface of several NSCLC cell lines have been examined, and H1299 cells were found to have the highest expression of CD44. When exposed to the micelle/CPT, the higher CD44-expressing H1299 cells showed lower cytotoxicity and apoptosis than the lower CD44-expressing CRL-5802 cells. To account for the higher therapeutic efficacy of CRL-5802 cells, experiments were conducted using endocytosis chemical inhibitors to understand if internalization of the micelle/CPT into the two cell lines involved different pathways and how this affected cell cycle arrest, apoptosis, and γ -H2AX formation. The *in vivo* biodistribution of the micelle in tumor-bearing mice was examined using a near-infrared optical imaging to determine the amount of micelles accumulated in the two tumors.

Materials and methods

Materials

Copper(I) bromide (CuBr), 3-(4,5-dimethyl-thiazol-2-yl)-2,5-diphenyl-tetrazolium bromide (MTT), propidium iodide (PI), sodium borate, Tween 20, dimethyl sulfoxide-*d* (DMSO-*d*₆), chloroform-*d* (CDCl₃) and deuterium oxide (D₂O) were purchased from Aldrich (St. Louis, MO). 2,2'-Bipyridine

(Bpy), 2-bromo-2-methylpropionyl bromide, Amberlite[®] IR120, Dowex 50W×8 (H) were purchased from Acros (Morris Plains, NJ). Chondroitin sulfate-g-poly(ϵ -caprolactone) copolymer containing a high content of poly(ϵ -caprolactone) (H-CP) and Rhodamine 123-conjugated H-CP (Rh123-H-CP) were prepared as previously described.⁶ Camptothecin (CPT) was kindly acquired from Industrial Technology Research Institute of Taiwan. Bovine serum albumin (BSA) was purchased from MDbio Inc. (Taipei, Taiwan). Fetal bovine serum (FBS) was purchased from Biological Industries (Beit Haemek, Israel). Dulbecco's modified Eagle's medium (DMEM) and Tris-glycine gels were purchased from Invitrogen (Carlsbad, CA). An annexin V-FITC apoptosis detection kit was purchased from Strong Biotech (Taipei, Taiwan). For western blot assay, the primary antibodies against XIAP, γ -H2AX and β -actin were purchased from Santa Cruz Biotechnology (Santa Cruz, CA), and primary antibodies against p27^{Kip-1}, CDK2 and cyclin A were purchased from GenTex Inc. (Irvine, CA).

Preparing H-CP micelle

A H-CP copolymer was synthesized according to our previous publication.⁶ The H-CP micelle was prepared by a simple dialysis method. Briefly, the H-CP copolymer (10 mg) was dispersed in 5 mL of DMSO containing 4 μ L of trifluoroacetic acid at 60 °C. The solution was placed in a dialysis bag (Mw cut-off 1000 membrane, Spectrum Labs, Rancho Dominguez, CA) and dialyzed against DD water for 1 day, followed by freeze-drying to produce the micellar product.

CPT or IR780-encapsulated micelles (micelle/CPT or micelle/IR780)

The method for preparing CPT or IR780-loaded micelles was similar to that for preparing the H-CP micelle. In brief, CPT or IR780 powder was dissolved in DMSO at 1 mg/mL to yield a stock solution. The H-CP (10 mg) powder was dissolved in 5 mL of DMSO containing 4 μ L of trifluoroacetic acid at 60 °C, followed by adding 1 mL of the CPT or IR780 stock solution. The solution was dialyzed against DD water using Mw cut-off 6000 membrane (Spectrum Labs, Rancho Dominguez, CA) for 1 day and then filtered to remove the unencapsulated CPT or IR780. Finally, the micelle/CPT or micelle/IR780 was obtained by freeze-drying.

Cell lines

CRL-5802 and H1299 non-small cell lung carcinoma cell lines were obtained from Dr. Cheng at the Biomedical Science and Environmental Biology Department of Kaohsiung Medical University in Taiwan and cultured in DMEM supplemented with 10% FBS and 1% penicillin-streptomycin at 37 °C under humidified 5% CO₂.

Expression of CD44 receptor

An immuno-phenotype analysis was used to evaluate the expression of CD44 receptor in several cell lines.¹¹ The cells of 5×10^5 cells/tube were suspended with 90 μ L PBS in 1.5 mL Eppendorf tubes and 10 μ L of CD44-FITC (50 μ g/mL) (eBioscience, San Diego, CA) was added to co-incubate at 4°C for 30 minutes in darkness. The cells were washed three times with 0.1M PBS and resuspended in 1 mL PBS. The fluorescence intensity of FITC was measured using flow cytometry (Becton-Dickinson,

Mansfield, MA). Data were averaged from three experiments.

Cytotoxicity

The cytotoxicities of CPT and micelle/CPT were measured using the MTT assay. The CPT powder was dissolved in DMSO to yield a stock solution (2 mg/mL), followed by dilution to a concentration of 0.0025 – 5.0 µg/mL in DMEM containing 10% FBS for the cytotoxic test of CPT. The equivalent CPT concentration of the micelle/CPT was controlled within 0.0025 – 5.0 µg/mL as well. Cells were seeded in 96-well culture plates at a density of 5×10^3 cells per well in DMEM containing 10% FBS for 24 hours. The culture medium was replaced with 100 µL medium containing various concentrations of CPT. Following 24 hours, the cells were washed three times with 0.1M PBS and replenish fresh medium to post-incubate for another 24 or 48 hours. The number of viable cells was measured by estimating their mitochondrial reductase activity using the tetrazolium-based colorimetric method.

Intracellular uptake and endocytosis inhibition

The synthesis of rhodamine 123-conjugated H-CP (Rh123-H-CP) was referred to our previous publication.⁶ The cellular uptake of Rh123-H-CP was studied using a flow cytometer. CRL-5802 or H1299 cells were seeded at a density of 2×10^5 cells per well in 6-well plates in DMEM supplemented with 10% FBS and incubated for 24 hours. The culture medium was removed and replaced with 2 mL DMEM containing Rh123-H-CP (100 µg/mL). The cells containing Rh123-H-CP were incubated at 37 °C for another 30 minutes or 2 hours. The cells were washed three times with 0.1M PBS, collected and

analyzed using the flow cytometer.

Three chemical inhibitors were utilized to study endocytosis pathways using following concentrations: wortmannin (50 nM), chlorpromazine (0.5, 1.0, 5.0 and 10 $\mu\text{g}/\text{mL}$), and genistein (50, 100 and 200 μM).¹² CRL-5802 or H1299 cells were seeded at a density of 1×10^5 cells per well in 6-well plates in DMEM supplemented with 10% FBS and incubated for 24 hours. The cells were pretreated with various concentrations of inhibitors at 37 °C for 30 minutes. Next, the cells were washed and replaced with 2 mL DMEM containing Rh123-H-CP (100 $\mu\text{g}/\text{mL}$). The cells were further incubated at 37 °C for 2 hours, washed three times with 0.1M PBS, collected, and analyzed using flow cytometry.

Cell cycle analysis

The effect of CPT and micelle/CPT internalization on cycle progression of cancer cells were studied by cell cycle analysis. Cells (CRL-5802 or H1299) were seeded at a density of 2×10^5 cells per well in 6-well plates and incubated in DMEM supplemented with 10% FBS for 24 hours. Subsequently, CPT and micelle/CPT were respectively added to the cells at an equivalent CPT concentration of 0.1 $\mu\text{g}/\text{mL}$ in the same culture medium. The cells containing the drug were then incubated at 37 °C for 24 hours.

The culture mediums were removed and the cells were washed and detached using 0.1% 1X trypsin (1 mL/well). The cells were collected by centrifugation at 1000 rpm for 5 minutes and fixed using 70% ethanol overnight. Following fixation, the cells were washed and incubated with 20 $\mu\text{g}/\text{mL}$ PI and 20

$\mu\text{g/mL}$ RNase in 0.1M PBS at room temperature for 15 minutes. The pellets of cells were obtained by centrifugation at 1000 rpm for 5 minutes and resuspended in 0.1M PBS to analyze the distribution of cell cycle using flow cytometry.

Cell apoptosis

To estimate the apoptosis-inducing efficiency of CPT and micelle/CPT, the annexin-V/PI dual staining assay was utilized. The cells were plated at a density of 2×10^5 cells per well into 6-well culture plates and incubated in DMEM containing 10% FBS for 24 hours. Next, the cells were respectively treated with CPT and micelle/CPT at a CPT concentration of 0.1 $\mu\text{g/mL}$ in DMEM without 10% FBS at 37 °C for 24 hours. The H-CP micelle and cultured cells were used as blank and control groups, respectively. The cells were washed three times with 0.1M PBS, collected and labeled with annexin V-FITC (10 $\mu\text{g/mL}$) and PI (20 $\mu\text{g/mL}$) at 37 °C for 30 minutes. After labeling, the cells were analyzed using flow cytometry. The experiment was repeated three times.

Evaluation of γ -H2AX activation

The degree of DNA damage was assessed using γ -H2AX as a marker.¹³ Cells were seeded at a density of 2×10^5 cells/well in 6-well tissue culture plates and incubated in DMEM medium containing 10% FBS for 24 hours. CPT and micelle/CPT was respectively added at a CPT concentration of 0.1 $\mu\text{g/mL}$ in the culture medium and then incubated at 37 °C for 24 hours. The cells were washed and harvested using 0.1% 1X trypsin (1 mL/well), collected into Eppendorf tubes and centrifuged at 3000 rpm for 10

minutes. Next, 70% ethanol was added dropwise into the tubes to fix the cells at -20 °C overnight. After fixation, the cells were washed in BSA-T-PBS solution (1% bovine serum albumin and 0.2% Triton X-100 in PBS; Sigma, St. Louis, MO) and incubated with 100 mL of the BSA-T-PBS solution containing 0.2 mg p-histone H2AX (Ser 139) monoclonal antibody (#sc-101696, Santa Cruz Biotechnology, Santa Cruz, CA) on a shaker at 4 °C overnight. Following centrifugation, the supernatant was discarded from the tubes and the residue was washed twice in the BSA-T-PBS solution. Alexa Fluor 488-tagged secondary antibody (Jackson Laboratory, Bar Harbor, ME) was diluted to 1:200 with the BSA-T-PBS solution and mixed with the cells at 37 °C for 1 hour. Following two washes with the BSA-T-PBS solution, the cells were incubated with 20 µg/mL of PI at room temperature for 30 minutes. The fluorescent intensity of the cells was recorded using flow cytometry.

Western blot analysis

CRL-5802 or H1299 cells were plated at a density of 2×10^5 cells per well into 6-well culture plates and incubated in DMEM (1mL) containing 10% FBS for 24 hours. The cells were respectively treated with CPT and micelle/CPT at a CPT concentration of 0.1 µg/mL and at 37 °C for 1 hour. The cells were scraped and collected to 1.5 mL Eppendorf tubes, and proteins were extracted from the cells by mixing with lysis buffer (0.05 mol/L Tris-HCl at pH 6.8, 2% SDS, and 6% β-mercaptoethanol) in ice for 30 minutes. Following lysis, the supernatant solution was separated from the cell pellets by centrifugation at 13,000 rpm for 30 minutes and the protein concentration was measured using a

BCATM protein assay kit (Pierce, Rockford, IL). Next, each protein (30 μg) was mixed with a 5X sample dye followed by boiling it at 95 °C for 5 minutes. An equal amount of protein (30 μg) was separated using 10% SDS-PAGE gel and transferred to a PVDF membrane. The PVDF (polyvinylidene difluoride; Merck Millipore Life Science, Darmstadt, Germany) membrane was blocked in blocking buffer (5% nonfat milk powder dissolved in Tris-buffered saline buffer containing 0.1% Tween 20 [TBST]) at room temperature. Following 1 h of incubation, the blocked PVDF membrane was probed with a 1:1000 dilution of phosphorylated histone H2AX, γ -H2AX (Ser¹³⁹) primary antibody in 1% nonfat milk-TBST buffer at 4 °C overnight. The next day, the PVDF membrane was washed three times with TBST and incubated with 1:4000 dilution of a horseradish peroxidase (HRP)-conjugated secondary antibody (Thermo Fisher Scientific, San Jose, CA) in TBST at room temperature for 1 h. The PVDF membrane was washed three times with TBST and developed using an enhanced chemiluminescence (ECL) detection kit (Amersham, Piscataway, NJ).

Confocal laser scanning microscopy (CLSM)

CRL-5802 or H1299 cells were seeded at a density of 1×10^5 cells per well in 12-well plates containing one glass coverslip per well, in DMEM supplemented with 10% FBS for 24 hours. The culture medium was replaced with 1 mL medium without 10% FBS, which contains either CPT or micelle/CPT at a CPT concentration of 0.1 $\mu\text{g}/\text{mL}$. The H-CP micelle (blank) and cultured cells were used as control groups. The cells with or without CPT were incubated at 37 °C for 24 hours. The

coverslips containing the cells were removed, washed gently twice with PBS, and then treated with 4% paraformaldehyde to fix cells for 30 minutes. After fixing, the cells on the coverslips were washed twice with PBS and then incubated with blocking buffer (1% BSA in PBS) at room temperature for 15 minutes. The supernatant was removed and then the cells were mixed with p-histone H2AX (Ser¹³⁹) monoclonal primary antibody (dilution 1: 300 with blocking buffer) at room temperature. Following 1 hour of standing, the cells on coverslips were washed 3 times with blocking buffer and stained with Alexa Fluor 488-tagged secondary antibody, which was diluted to 1: 200 with the blocking buffer and incubated at 37 °C for 1 hours. Following two washes with the blocking buffer, the coverslips containing the cells were mounted with Fluoromount-GTM (eBioscience) for CLSM observation (Olympus Fv 1000, Tokyo, Japan).

***In vivo* biodistribution**

Nude mice (Balb/cAnN.Cg-*Foxn1*^{fl^u}/CrINarl, male, ~ 6 weeks old) were purchased from National Laboratory Animal Center (NLAC) of Taiwan. The animal experiment was approved by Institutional Animal Care and Use, Committee of Kaohsiung Medical University. The biodistribution of micelle/IR780 was monitored by non-invasive fluorescence in tumor-bearing mice with two tumors grafted on the right (H1299) and left (CRL-5802) hind legs. After tumors grew to approximately 150 mm³ in volume, the micelle/IR780 (1.75 mg/kg of IR780) was intravenously injected via the lateral tail vein into tumor-bearing mice.¹⁴ Following the injection, the micelle/IR780 was imaged at several time

points (1, 4, 8, 12, 24, 36 and 48 hours) using an IVIS Spectrum System 3D (Caliper Life Sciences, Hopkinton, MA). The exposure time was set at 2 seconds and the wavelength of excitation and emission was selected at 745nm and 840nm with an ICG filter. Following 48 hours, relevant organs, tissues, and tumors were harvested from the mice and imaged immediately to quantify intensities using the region of interest (ROI) function of the Living Image[®] software and then the heart, liver and kidney were sectioned into slices for histopathological examination with Hematoxylin & Eosin (H&E) staining.

Statistical analysis

Means and standard deviations (SD) of data were calculated. Comparison between groups was tested using Student's *t*-test and $P < 0.05$ was considered to be significant.

Results and discussion

CD44 expression and cytotoxicities

A chondroitin sulfate-*g*-poly(ϵ -caprolactone) copolymer with a high content of PCL (18.7 mol%), named H-CP, had been synthesized and utilized to encapsulate the hydrophobic CPT (micelle/CPT) in the core for tumor-targeting delivery.⁶ With recognition of the H-CP micelle to CD44, the micelle/CPT entered CRL-5802 cells and released CPT efficaciously, thus showing higher tumor suppression compared with the commercial CPT-11. Examination of CD44 expression on the surface of many

NSCLCs revealed that H1299 cells show higher CD44 expression than CRL-5802 cells (Figure 1).

Thus, it was hypothesized that the therapeutic outcome of CPT released from the micelle/CPT against H1299 cells should be better than that against CRL-5802 cells.

To test this hypothesis, the cell viabilities of the two cell lines exposed to free CPT and the micelle/CPT were promptly screened after 24 and 48 hours of incubation (Figure 2). The cytotoxicities of the micelle/CPT were found to be higher than that of free CPT in both cell lines and after both incubation durations. The anticancer drug-encapsulated NPs usually have advantages over their parent drugs including: (1) an increase in water solubility of low soluble or insoluble anticancer drugs and an enhancement in biodistribution and therapeutic efficacy; (2) an accumulation of anticancer drugs in tumor tissues by the enhanced permeation and retention (EPR) effect and a reduction in systemic side effects; (3) protection of anticancer drugs against deactivation during blood circulation, transport to targeted organs or tissues and intracellular trafficking. In CRL-5802 cells, the micelle/CPT showed higher potency in cell-killing activity (IC_{50} = 0.01 μ g/mL for 24 hours, IC_{50} = 0.004 μ g/mL for 48 hours) than in H1299 cells (IC_{50} = 1.36 μ g/mL for 24 hours, IC_{50} = 0.15 μ g/mL for 48 hours). This result completely contradicted the hypothesis that higher CD44 expression on H1299 cell membrane should enhance the cellular uptake of the micelle/CPT, leading to better therapeutic outcome of CPT.

Intracellular uptake and endocytosis inhibition

To further confirm the hypothesis, flow cytometry was utilized as an alternative measurement to

examine the internalization efficacy of the H-CP micelle into two cell lines. A fluorescent dye, rhodamine 123 (Rh123), was conjugated to the micelle. As seen in Figure 3 (A&B), the cellular uptake of the Rh123-H-CP micelle into CRL-5802 cells was profoundly higher than that into H1299 for 30 minutes and for 2 hours of incubation. This result agreed with the finding in cytotoxicity (Figure 2). The higher CD44-expressing H1299 cells were less able to internalize the micelle, which may be attributed to other pathways, besides the CD44-mediated endocytosis, involved in uptake of the micelle in the two cell lines.

Different endocytosis pathways of nanomedicine involved in cellular uptake have been widely reported.¹⁵ Thus, the cells were pretreated with three chemical inhibitors before being treated with the Rh123-H-CP micelle. Wortmannin was selected for macropinocytosis; chlorpromazine, for clathrin-mediated endocytosis (CME); and genistein, for caveolae-mediated endocytosis.⁶ The inhibition effect of these three inhibitors on cellular uptake of the micelle was preliminarily tested at the following concentrations: 50 nM wortmannin, 10 µg/mL chlorpromazine, and 200 µM genistein. Flow cytometric diagrams showed a left shift when CRL-5802 and H1299 cells were respectively pretreated with chlorpromazine and genistein, indicating the inhibition effect, while the diagrams remained intact when the cells were treated with wortmannin (Supporting Figure 1S). Thus, the dose-dependent inhibition of chlorpromazine and genistein was further tested. Flow cytometric diagrams showed an apparent shift to the left when CRL-5802 cells were pretreated with

chlorpromazine at 5 and 10 $\mu\text{g}/\text{mL}$, and genistein at 100 and 200 μM , as compared with the control group (Supporting Figure 1S). Subsequently, the cellular accumulation of fluorescence intensity was quantified according to the control group. The fluorescence intensity decreased significantly for the chlorpromazine- and genistein-pretreated cells at the aforementioned concentrations (Figure 3C). The same test was done on H1299 cells. No inhibition effect was observed in H1299 cells pretreated with different doses of chlorpromazine. In contrast, there is an apparent shift to the left when the cells were pretreated with genistein at a low dose of 10 μM (Supporting Figure 1S and Figure 3D). The flow cytometric results suggest that the cellular uptake of the micelle was indeed cell line-dependent. The cellular uptake of the micelle into CRL-5802 cells utilized CD44-, clathrin-, and caveolae-mediated endocytosis; however, in H1299 cells, only CD44- and caveolae-mediated endocytosis pathways were involved.

Cellular internalization and subsequent intracellular processing of nanoparticles are key barriers to successful *in vitro* and *in vivo* delivery of drugs. Clathrin- and caveolin-dependent endocytosis have been extensively studied in the past decade.¹⁵ Clathrin-dependent endocytosis yields acidified vesicles (pH 5 - 6) that fuse with lysosomes (pH \sim 4.5). Caveolin-dependent uptake is less well characterized but is associated with the formation of caveosomes that are less acidified and are believed to avoid trafficking to lysosomes. The differences in endocytic vesicles and subsequent processing may significantly impact the intracellular destination of drug-encapsulated nanoparticles. There are several

examples in which CME appears to be defined as the most prominent mechanism for cellular entry.¹⁶⁻²⁰

For example, the nanoparticles made of D,L-poly(lactide (PLA) and poly(ethylene glycol-*co*-lactide) (PEG-*co*-PLA) have been explored for drug delivery. Owing to the presence of the partially hydrolyzed PLA, the surface of the nanoparticles was negatively charged and usually altered with cationic surfactants such as stearylamine.^{16, 21} In the polarized MDCK epithelial cells, the nanoparticles used CME independent of their charge. In contrast, in non-polarized HeLa cervical cancer cells, the anionic particles used multiple pathways (CME and caveolae-mediated), while cationic particles appeared to be restricted to CME and macropinocytosis. Hyaluronic acid (HA) conjugated with hydrophobic poly(L-histidine) (PHis) was utilized to prepare a pH-responsive and tumor-targeted copolymer, hyaluronic acid-g-poly(L-histidine) (HA-PHis), for use as a carrier for anti-cancer drugs.²² The results demonstrated the pH-responsive HA-PHis micelles were taken up via CD44 receptor-mediated endocytosis as well as via CME, and delivered to lysosomes, which contribute to trigger the release of doxorubicin (DOX) into the cytoplasm. A review of these examples showed that using the CME pathway seems to enhance cellular uptake of biodegradable micelles and results in better therapeutic outcome.

Cell cycle

CPT is a potent anticancer drug which inhibits DNA topoisomerase I and causes apoptosis of cancer cells.²³ To understand further the mechanism of drug action, the effect of CPT on the cell cycle of two

cell lines was evaluated. Cell cycle arrest was analyzed using propidium iodide (PI)-labeled RNase in CRL-5802 and H1299 cells after 24 hours of post-incubation. Flow cytometric analysis showed 21.3%, 40.4%, and 18.3% of arrest for CPT-treated CRL-5802 cells and 26.0%, 37.4%, and 13.0% for micelle/CPT-treated CRL-5802 cells in G₁, S and G₂-M phases, respectively (Figure 4A). Similarly, flow cytometric analysis was done on H1299 cells. There were 19.4%, 27.8%, and 45.3% of arrest for CPT-treated cells and 7.89%, 23.8%, and 58.8% for micelle/CPT-treated cells found in G₁, S, and G₂-M phases, respectively (Figure 4B). Cell cycle analysis revealed that CPT or micelle/CPT arrested mainly CRL-5802 cells in the S phase and H1299 cells in the G₂-M phase. Although CPT has been shown to induce an accumulation of cells at the intra-S-phase checkpoint,²⁴ other studies also showed that both low-dose CPT and CPT-resistant cancer cells could induce accumulations at G₁/S transition or G₂/M boundary instead of the intra-S arrest alone.²⁵ This fact will attenuate the therapeutic outcome of CPT.

The S-phase cells of the myelogenous leukemias HL-60 or KG-1 are susceptible to undergo apoptosis in the presence of CPT. However, glioma cells U-251 MG and D-54 MG which express ectopic p16 lead to G₁ phase arrest and are resistant to CPT derivative topotecan.²⁶ On the contrary, human lymphocytic leukemia cells MOLT-4 or mouse L1210 cells are resistant to CPT and no significant CPT-induced accumulation in S phase was detected.^{27, 28} In addition, Goldwasser's work showed that human colon cancer cell lines SW620 and KM12 trigger accumulations in two distinct

phases following CPT treatment.²⁵ The CPT-resistant KM12 was arrested in G₂, whereas the CPT-sensitive SW620 was arrested in S phase irreversibly. The effect of CPT on the cell cycle arrest was indeed cell line-dependent.

The S-phase selectivity reflects that the formation of double-strand DNA breaks when the advancing replication forks collide with CPT-stabilized topo I-DNA complexes.^{29, 30} Nevertheless, additional studies revealed that further exposure of exponentially growing cells to high CPT concentrations produces a subsequent G₂ arrest in synchronized HeLa cells as a consequence of impaired activation of cdc2-cyclin B complexes.^{31, 32} Their results suggested that the alteration in checkpoints of DNA damage may be a critical factor for defining the chemosensitivity of cancer cells to CPT.

p27^{Kip-1} is a member of Cip/Kip family and modulates the progression of cell cycle by binding cyclin/Cdk complexes. Furthermore, p27 acts as a regulator of cell cycle progression at both G₁/S and S to G₂/M transition phases.³³ In normal cells, p27 is a tumor suppressor and has been reported to inhibit the cell-cycle progression. However, the expression of p27 has been shown to be a negative indicator that correlated with the prognosis of patients with oral squamous cancer,³⁴ chronic B-cell lymphocytic leukemia,³⁵ and non-small cell lung cancer.³⁶ Here, the CPT/micelle causes a dramatically decreased level of p27 protein in CRL-5802 cells, but not in H1299 cells (Figure 4C). The down-regulation of p27 is presumed to enhance the cytotoxicity of CRL-5802 cells treated with the CPT/micelle.

Cell apoptosis

To examine the induction of cell apoptosis in the CPT-treated or micelle/CPT-treated cells at a CPT concentration of 0.1 $\mu\text{g}/\text{mL}$, an annexin-V/PI dual staining assay was conducted using flow cytometry (Figure 5A). The four quadrants display necrotic cells stained with PI in the first quadrant (Q1), late apoptotic cells stained with PI and annexin-V in the second quadrant (Q2), early apoptotic cells stained with annexin-V in the third quadrant (Q3), and healthy cells not stained with PI and annexin-V in the fourth quadrant (Q4). The quantification of apoptotic cells was plotted in Figure 5(B). The percentages of late/early apoptotic cells (Q2+Q3) of micelle/CPT-treated CRL-5802 cells ($\sim 34\%$) were significantly higher than that of CPT-treated cells ($\sim 25\%$); however, no significant difference was found in H1299 cells exposed to either micelle/CPT or CPT. The relative apoptosis ratios between cells treated with the micelle/CPT and empty H-CP in CRL-5802 and H1299 cells were calculated and plotted in Figure 5(C). The relative apoptosis ratio was about 3.5 for CRL-5802 cells and about 1.5 for H1299 cells. These results demonstrated the micelle/CPT has significantly higher cell-killing efficiency in CRL-5802 cells than in H1299 cells and using the micelle/CPT is more potent than using CPT against CRL-5802 cells.

Evaluation of γ -H2AX

The nucleus contains genomic materials (DNA and RNA), regulates the gene expression and controls the replication of DNA during the cell cycle. Hence, damaging the DNA in the nucleus of cancer cells

would lead to inhibition of rapid cellular division. The most common assay of DNA fragmentation relies on labeling DNA double-strand breaks (DSBs) with fluorochrome-tagged deoxynucleotides. The induction of DSBs by genotoxic agents provides a signal for histone H2AX phosphorylation on Ser¹³⁹; the phosphorylated H2AX is named γ -H2AX. Hence, γ -H2AX has evolved as one of the important biomarkers for observing DNA damage.³⁷

To understand the effect of CPT or micelle/CPT on the nucleus of CRL-5802 and H1299 cells, the cells were treated with the equivalent CPT concentration of 0.1 μ g/mL for 2 hours. The cells were stained with green fluorescent Alexa fluor 488 antibody specific for γ -H2AX and the expression of γ -H2AX was determined using flow cytometry, western blot analysis, and CLSM of cells exposed to H-CP, CPT, or micelle/CPT. As seen in the flow cytometric diagrams, the expression of γ -H2AX was profoundly high in both cells exposed to CPT and micelle/CPT as compared with the control group and H-CP-treated group (Figure 6A&B). In CRL-5802 cells, it was much clearer that micelle/CPT-treated cells induced a significantly higher level of γ -H2AX expression than CPT-treated cells. When the expression of γ -H2AX in micelle/CPT-treated cells was quantified, around 3-fold increase in γ -H2AX expression could be found in CRL-5802 as compared with that in H1299 cells (Figure 6B). Similar result was obtained from the western blot image (Figure 6C), illustrating a higher γ -H2AX expression in CRL-5802 cells than in H1299 cells. Table 1 summarizes the *in vitro* anticancer superiority of CRL-5802 cells over that of H1299 cells when the cells were exposed to micelle/CPT.

Figure 7 shows the expression of γ -H2AX evaluated by CLSM. As can be seen, invisible γ -H2AX expression was found in the nuclei of untreated CRL-5802 and H1299 cells, slightly visible expression in cells treated with empty H-CP, and highly visible expression in cells treated with CPT and micelle/CPT. Both CPT and micelle/CPT had higher ability in causing DNA damage in CRL-5802 cells than in H1299 cells because the higher intensity of green fluorescence indicates higher expression of γ -H2AX in the nucleus.

***In vivo* biodistribution**

To evaluate the *in vivo* accumulation of micelles in CRL-5802 and H1299 xenografted tumors, a near-IR dye, IR780, was encapsulated into micelles. The biodistribution of micelle/IR780 was monitored by non-invasive fluorescence in tumor-bearing mice with the tumor grafted on the right (H1299) and left (CRL-5802) hind legs. After tumors grew to approximately 150 mm³ in volume, the micelle/IR780 was intravenously injected via the lateral tail vein into tumor-bearing mice.¹⁴ Following the injection, the micelle/IR780 was imaged at different time points as shown in Figure 8(A). The fluorescence intensity of IR780 at both tumor sites increased with increasing circulation time. It was clear the fluorescence intensity is always higher on the CRL-5802 tumor than on the H1299 tumor in mice if compared at the same time points. To confirm whether the higher accumulation of the micelle/IR780 on the CRL-5802 tumor was due to the different tumor sizes, tumors were isolated after 48 hours. The image of Figure 8(B) illustrates clearly tumors of similar sizes. The relevant organs,

tissues, and tumors were also dissected from mice at 48 hours after instillation and optically imaged immediately to determine the remaining fluorescence intensity. In Figure 8(C), high IR780 fluorescence intensities were observed at both tumor sites because of enhanced permeation and retention (EPR) effect.³⁸ The optical imaging intensity of the CRL-5802 tumor was significantly higher than that of the H1299 tumor (Figure 8D), indicating that the CLR-5802 tumor indeed had higher ability in internalization of the micelle. To evaluate the safety of the H-CP micelle *in vivo*, the heart, liver, and kidney were harvested for histopathological examination with Hematoxylin & Eosin (H&E) staining as well. Neither noticeable organ damage nor inflammation was observed in the micelle/IR780 group compared with the saline group (Figure 8E).

Conclusions

This study demonstrated why lower CD44-expressing CRL-5802 cells caused higher DNA damage and higher cellular uptake as compared with higher CD44-expressing H1299 cells when exposed to CPT or micelle/CPT. Endocytic chemical inhibitors were utilized to examine the internalization pathways of the micelle/CPT into the cells. CRL-5802 cells involved CD44-, clathrin-, and caveolae-mediated pathways, while H1299 cells involved only CD44- and caveolae-mediated pathways. Using CME seems to be superior because micelles encapsulated with endosomes could reach the acidic lysosomes, where the abundance of enzymes helps degrade the H-CP micelle and accelerate the release of CPT.

From the cell cycle analysis of CPT-treated cells, CRL-5802 cells arrested mainly in the S phase and

H1299 cells, mainly in the G₂-M phase. The qualitative and/or quantitative evaluation of γ -H2AX expression, a biomarker for DNA damage, was obtained from flow cytometry, CLSM, and western blot studies. All results demonstrated that CRL-5802 cells had higher γ -H2AX expression than H1299 cells. The *in vivo* biodistribution of micelle/IR780 in tumor-bearing mice showed that the CRL-5802 tumor had higher fluorescence intensity than the H1299 tumor. It can be concluded that the therapeutic outcome of a drug does not correlate only with the amount of CD44 on the surface of cancer cells. The cells used multiple internalization pathways and arrested in the S phase as demonstrated in CRL5802 cells, showing a higher ability in causing cell death as compared with H1299 cells.

Acknowledgements

We are grateful for the financial support from the Ministry of Science and Technology of Taiwan (MOST103-2325-B-037-001 and MOST103-2320-B-037-012-MY3). This study is also supported by "Aim for the Top 500 Universities Grant (KMU-DT103007)" and by "NSYSU-KMU Joint Research Project, (NSYSUKMU 104-P026)" from Kaohsiung Medical University. We appreciate the experiment support of a confocal laser scanning microscope and an optical imaging system from Center for Research Resources and Development of KMU.

References

1. F. Li and K. Na, *Biomacromolecules*, 2011, **12**, 1724-1730.
2. F. Ronca, L. Palmieri, P. Panicucci and G. Ronca, *Osteoarthritis Cartilage*, 1998, **6 Suppl A**, 14-21.
3. R. Bagari, D. Bansal, A. Gulbake, A. Jain, V. Soni and S. K. Jain, *J. Drug Targeting*, 2011, **19**, 251-257.
4. D. Naor, R. V. Sionov and D. Ish-Shalom, in *Adv. Cancer Res.*, eds. F. V. W. George and K. George, Academic Press, 1997, Volume 71, pp. 241-319.
5. H. A. Kargi, M. F. Kuyucuoglu, M. Alakavuklar, O. Akpinar and S. Erk, *Cancer Lett.*, 1997, **119**, 27-30.
6. Y. S. Liu, C. C. Chiu, H. Y. Chen, S. H. Chen and L. F. Wang, *Mol. Pharm.*, 2014, **11**, 1164-1175.
7. O. M. Koo, I. Rubinstein and H. Onyuksel, *Nanomedicine*, 2005, **1**, 77-84.
8. Q. Y. Li, Y. G. Zu, R. Z. Shi and L. P. Yao, *Curr. Med. Chem.*, 2006, **13**, 2021-2039.
9. E. K. Park, S. B. Lee and Y. M. Lee, *Biomaterials*, 2005, **26**, 1053-1061.
10. G. Pasut and F. M. Veronese, *Adv. Drug Deli. Rev.*, 2009, **61**, 1177-1188.
11. X. Y. Zhu, X. Z. Zhang, L. Xu, X. Y. Zhong, Q. Ding and Y. X. Chen, *Biochem. Biophys. Res. Commun.*, 2009, **379**, 1084-1090.
12. S. F. Peng, C. J. Su, M. C. Wei, C. Y. Chen, Z. X. Liao, P. W. Lee, H. L. Chen and H. W. Sung, *Biomaterials*, 2010, **31**, 5660-5670.
13. C.-C. Chiu, J.-W. Haung, F.-R. Chang, K.-J. Huang, H.-M. Huang, H.-W. Huang, C.-K. Chou, Y.-C. Wu and H.-W. Chang, *PLoS One*, 2013, **8**, e64739.
14. C. L. Peng, Y. H. Shih, P. C. Lee, T. M. Hsieh, T. Y. Luo and M. J. Shieh, *ACS Nano*, 2011, **5**, 5594-5607.
15. G. Sahay, D. Y. Alakhova and A. V. Kabanov, *J. Control. Release*, 2010, **145**, 182-195.
16. O. Harush-Frenkel, N. Debotton, S. Benita and Y. Altschuler, *Biochem. Biophys. Res. Commun.*, 2007, **353**, 26-32.
17. W. Li, C. Chen, C. Ye, T. Wei, Y. Zhao, F. Lao, Z. Chen, H. Meng, Y. Gao, H. Yuan, G. Xing, F. Zhao, Z. Chai, X. Zhang, F. Yang, D. Han, X. Tang and Y. Zhang, *Nanotechnology*, 2008, **19**, 145102.
18. J. Z. Rappoport, *Biochem. J.*, 2008, **412**, 415-423.
19. P. J. Smith, M. Giroud, H. L. Wiggins, F. Gower, J. A. Thorley, B. Stolpe, J. Mazzolini, R. J. Dyson and J. Z. Rappoport, *Int. J. Nanomed.*, 2012, **7**, 2045-2055.
20. G.-J. Chen, C. Hsu, J.-H. Ke and L.-F. Wang, *J. Biomed. Nanotech.*, 2015, **11**, 951-963.
21. O. Harush-Frenkel, E. Rozentur, S. Benita and Y. Altschuler, *Biomacromolecules*, 2008, **9**, 435-443.

22. L. Qiu, Z. Li, M. Qiao, M. Long, M. Wang, X. Zhang, C. Tian and D. Chen, *Acta biomaterialia*, 2014, **10**, 2024-2035.
23. M. E. Wall, M. C. Wani, C. E. Cook, K. H. Palmer, A. T. McPhail and G. A. Sim, *J. Amer. Chem. Soc.*, 1966, **88**, 3888-3890.
24. J. A. Seiler, C. Conti, A. Syed, M. I. Aladjem and Y. Pommier, *Mole. Cell. Biol.*, 2007, **27**, 5806-5818.
25. F. Goldwasser, T. Shimizu, J. Jackman, Y. Hoki, P. M. O'Connor, K. W. Kohn and Y. Pommier, *Cancer Res.*, 1996, **56**, 4430-4437.
26. J. Fueyo, C. Gomez-Manzano, V. Puduvalli, P. Martin-Duque, R. Perez-Soler, V. Levin, W. Yung and A. Kyritsis, *Int. J. Oncol.*, 1998, **12**, 665-674.
27. W. A. Cliby, K. A. Lewis, K. K. Lilly and S. H. Kaufmann, *J. Biol. Chem.*, 2002, **277**, 1599-1606.
28. Z. Darzynkiewicz, S. Bruno, G. Del Bino and F. Traganos, *Ann. NY Acad. Sci.*, 1996, **803**, 93-100.
29. A. J. Ryan, S. Squires, H. L. Strutt and R. T. Johnson, *Nucleic Acids Res.*, 1991, **19**, 3295-3300.
30. K. Avemann, R. Knippers, T. Koller and J. M. Sogo, *Mol. Cell. Biol.*, 1988, **8**, 3026-3034.
31. Y.-P. Tsao, P. D'Arpa and L. F. Liu, *Cancer Res.*, 1992, **52**, 1823-1829.
32. R. A. Tobey, *Cancer Res.*, 1972, **32**, 2720-2725.
33. A. Martín, J. Odajima, S. L. Hunt, P. Dubus, S. Ortega, M. Malumbres and M. Barbacid, *Cancer Cell*, 2005, **7**, 591-598.
34. M. Zhang, J. Li, L. Wang, Z. Tian, P. Zhang, Q. Xu, C. Zhang, F. Wei and W. Chen, *Oncol. Lett.*, 2013, **6**, 381-386.
35. R. Vrhovac, A. Delmer, R. Tang, J.-P. Marie, R. Zittoun and F. Ajchenbaum-Cymbalista, *Blood*, 1998, **91**, 4694-4700.
36. W. Sterlacci, M. Fiegl, W. Hilbe, H. Jamnig, W. Oberaigner, T. Schmid, F. Augustin, J. Auberger, E. C. Obermann and A. Tzankov, *J. Thoracic. Oncol.*, 2010, **5**, 1325-1336.
37. J. Dickey, C. Redon, A. Nakamura, B. Baird, O. Sedelnikova and W. Bonner, *Chromosoma*, 2009, **118**, 683-692.
38. H. Maeda and Y. Matsumura, *Adv. Drug Deliv. Rev.*, 2011, **63**, 129-130.

Caption Legends

Fig. 1. Fluorescent intensities of CD44 expression in non-small cell lung cancer cell lines and U87 cells (a human glioblastoma cell line).

Fig. 2. Cell viability tests of CPT and CPT-loaded micelle (micelle/CPT) against (A) CRL-5802 cells and (B) H1299 cells for 24 and 48 hours of incubation using an MTT assay.

Fig. 3. Flow cytometric histograms of CRL-5802 and H1299 cells exposed to Rh123-linked micelle for (A) 30 minutes and (B) 2 hours of incubation. The inhibition of intracellular uptake in (C) CRL-5802 cells and (D) H1299 cells pretreated with dose-dependent chlorpromazine and genistein inhibitors for 30 minutes before the cells were exposed to the micelle for 2 hours of incubation.

Fig. 4. Cell cycle analysis of H-CP, CPT, and micelle/CPT against (A) CRL-5802 cells and (B) H1299 cells for 24 hours of incubation using the equivalent CPT concentration of 0.1 $\mu\text{g}/\text{mL}$. (C) The protein-expression amounts of cell cycle modulators p27, CDK2 and cyclin A, and pro-survival protein XIAP. The results of western blot analysis showed that the micelle/CPT causes a dramatically decreased level of p27 protein in CRL-5802 cells as compared with H1299 cells. β -Actin was used as an internal control for equal loading.

Fig. 5. Induction of apoptosis in CRL-5802 and H1299 cells exposed to H-CP micelle, CPT, and micelle/CPT for 24 hours of incubation at 37 $^{\circ}\text{C}$ using the equivalent CPT concentration of 0.1 $\mu\text{g}/\text{mL}$. (A) the annexin-V/PI dual staining assay, (B) the percentage of apoptosis cells calculated from (A). (C) The relative apoptosis ratios between cells treated with the micelle/CPT and empty H-CP (n=3, *P< 0.05).

Fig. 6. Formation of γ -H2AX in (a) CRL-5802 cells and (b) H1299 cells exposed to micelle, free CPT, and micelle/CPT for 2 hours of incubation using the equivalent CPT concentration of 0.1 $\mu\text{g}/\text{mL}$. (A) The expression of γ -H2AX was analyzed by flow cytometry, (B) plotted in percentage of γ -H2AX-positive cells, and (C) done by western blotting analysis (n=3, *P< 0.05). β -Actin was used as an internal control for equal loading.

Fig. 7. CLSM images of γ -H2AX in CRL-5802 and H1299 exposed to micelle, free CPT, and micelle/CPT for 2 hours of incubation using the equivalent CPT concentration of 0.1 $\mu\text{g}/\text{mL}$. The cells nuclei were stained with DAPI in blue and γ -H2AX was stained with p-histone H2AX (Ser 139) monoclonal primary antibody and Alexa Fluor 488-tagged secondary antibody. The formation of γ -H2AX foci was indicated in green fluorescence.

Fig. 8. (A) The optical images of CLR-5802 and H1299 tumors xenografted in male Balb/c mice (~ 6 weeks old, n=3 labeled as #1, 2, 3) using a near-infrared non-invasive optical imaging technique. (B) The tumors isolated to validate similar sizes. (C) The fluorescent images and (D) relative fluorescence intensities of isolated tissues after mice were injected with the IR-780-loaded micelle (micelle/IR 780)

for 48 hours. (E) HE analysis of the effect of the micelle on heart, liver, and kidney. (The equivalent concentration of IR780 is 1.75 mg/kg using EX 745 nm and EM 840 nm).

Table 1. The summary of the *in vitro* data obtained from the study in two cell lines

		CRL-5802	H1299
CD 44 expression		Low	High
IC₅₀ (micelle/CPT)	24 hr	0.01 µg/mL	1.36 µg/mL
	48 hr	0.004 µg/mL	0.15 µg/mL
Endocytosis pathways		clathrin- and caveolae-	caveolae-
Cell cycle		S phase	G ₂ -M phase
Cell apoptosis (micelle/CPT)		33.06 ± 2.49 %	14.14 ± 2.68 %
γ-H2AX (micelle/CPT)		High	Low

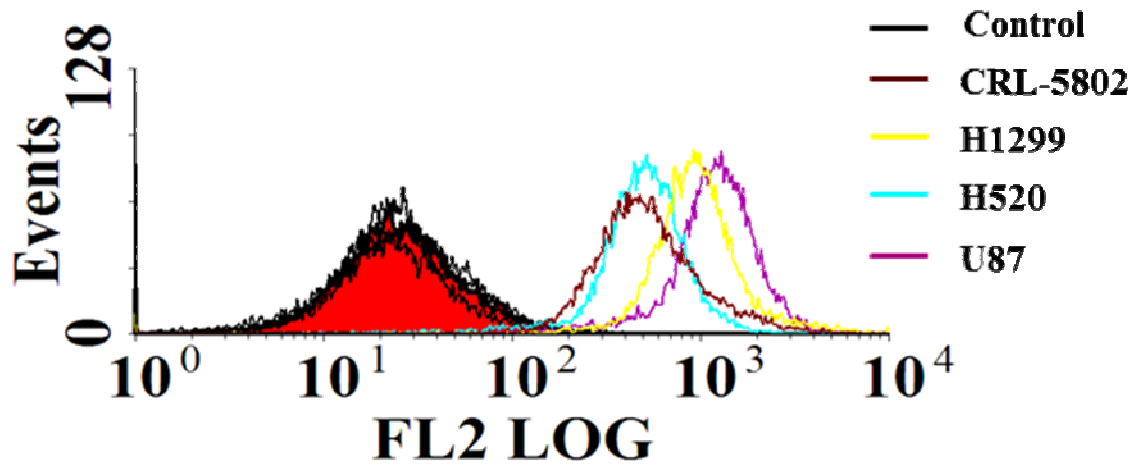


Fig. 1. Fluorescent intensities of CD44 expression in non-small cell lung cancer cell lines and U87 cells (a human glioblastoma cell line).

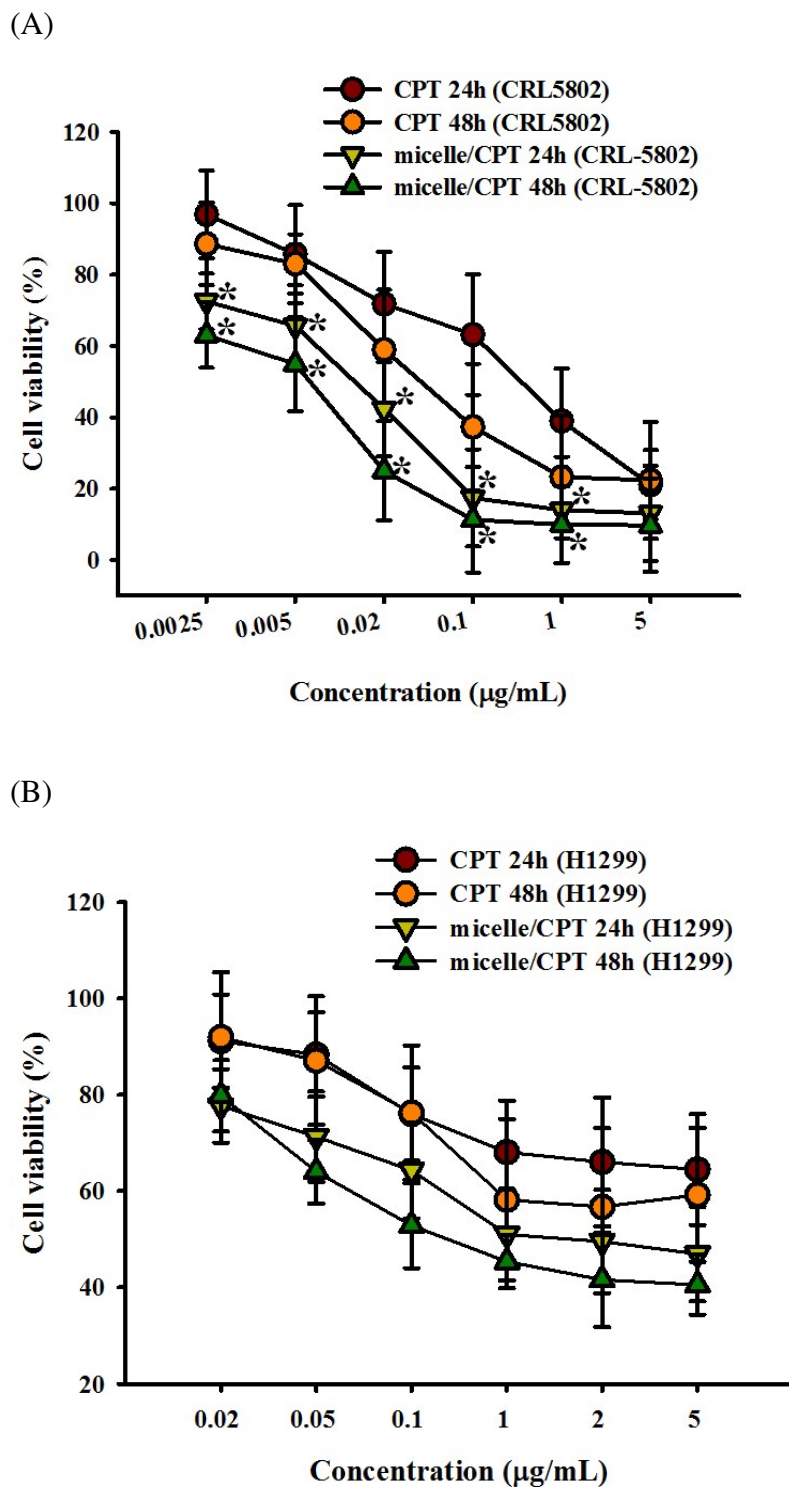


Fig. 2. Cell viability tests of CPT and CPT-loaded micelle (micelle/CPT) against (A) CRL-5802 cells and (B) H1299 cells for 24 and 48 hours of incubation using an MTT assay.

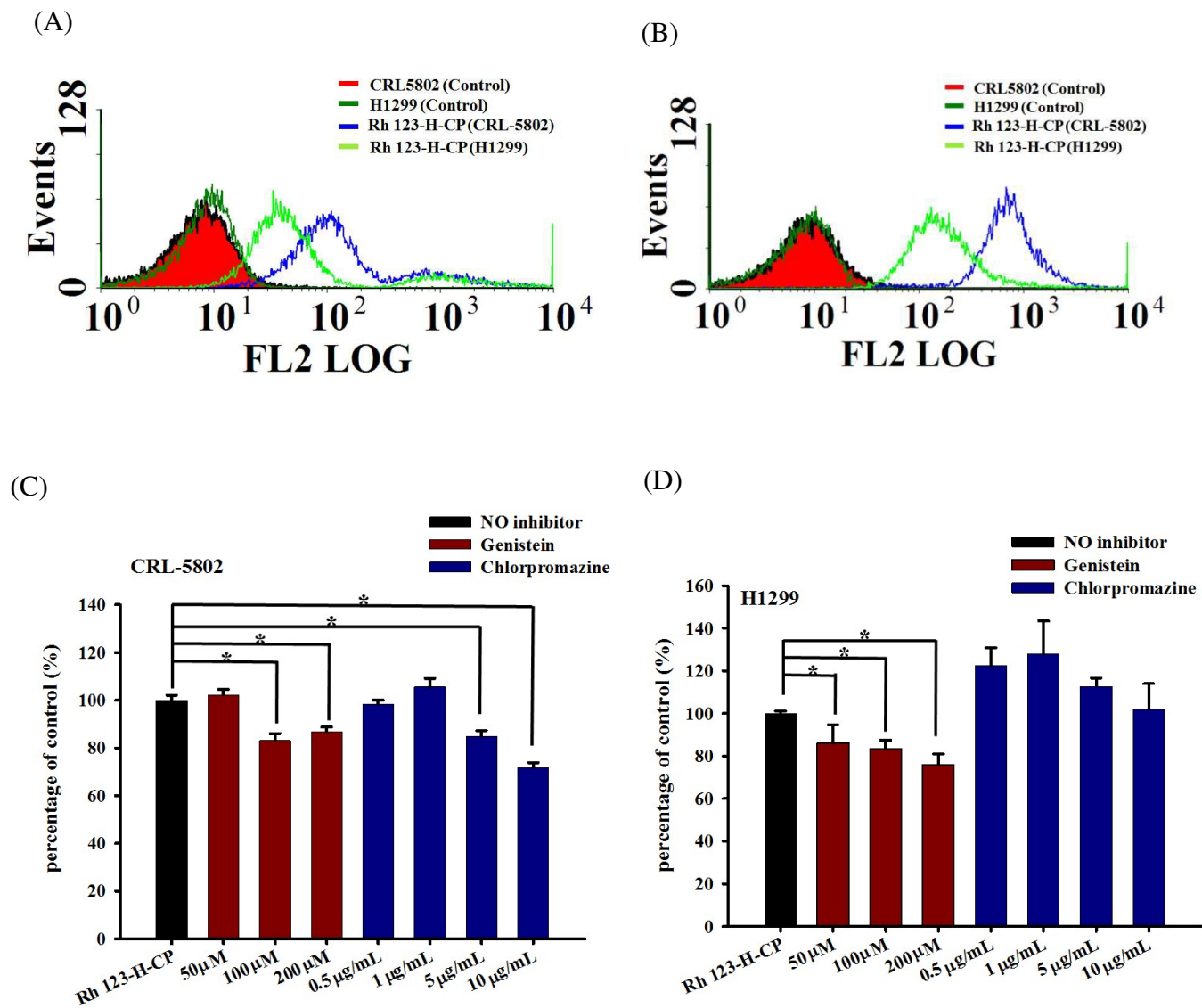
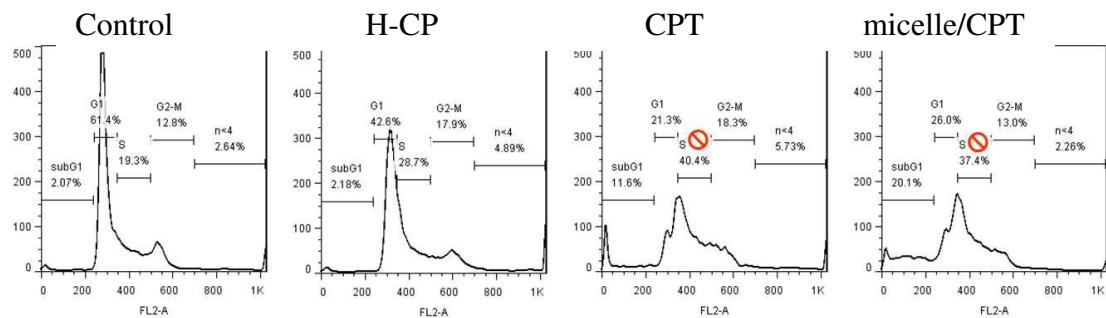
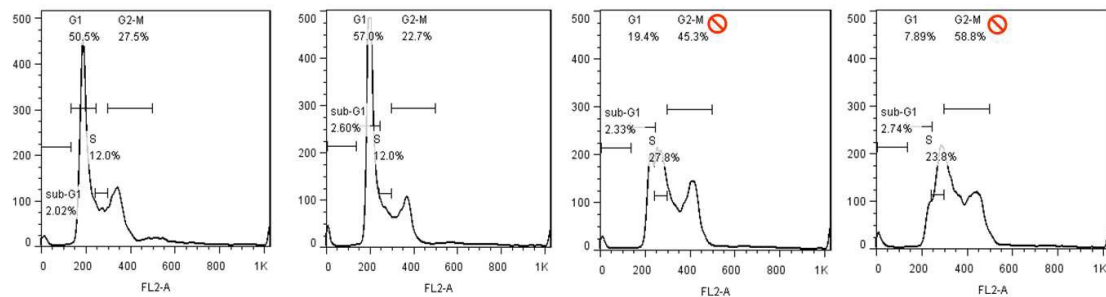


Fig. 3. Flow cytometric histograms of CRL-5802 and H1299 cells exposed to Rh123-linked micelle for (A) 30 minutes and (B) 2 hours of incubation. The inhibition of intracellular uptake in (C) CRL-5802 cells and (D) H1299 cells pretreated with dose-dependent chlorpromazine and genistein inhibitors for 30 minutes before the cells were exposed to the micelle for 2 hours of incubation.

(A) CRL-5802



(B) H1299



(C)

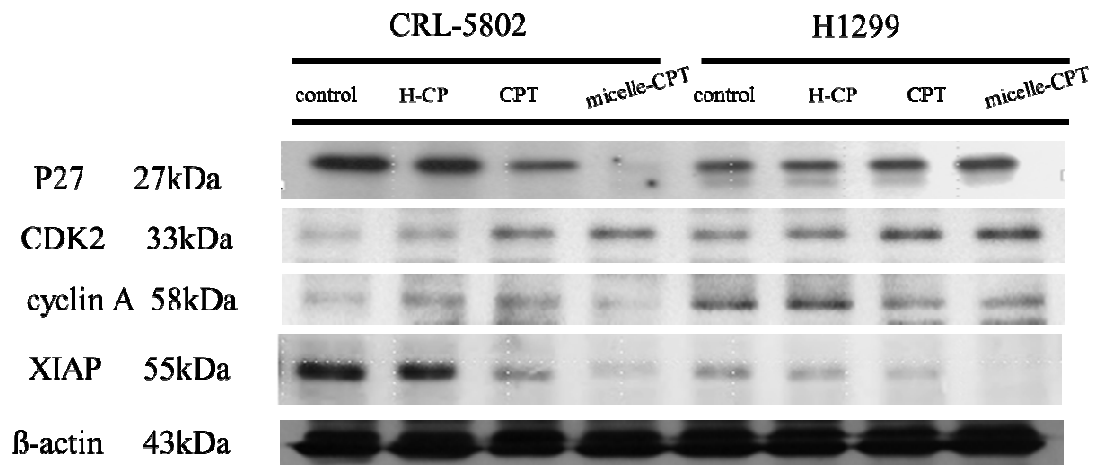


Fig. 4. Cell cycle analysis of H-CP, CPT, and micelle/CPT against (A) CRL-5802 cells and (B) H1299 cells for 24 hours of incubation using the equivalent CPT concentration of 0.1 $\mu\text{g}/\text{mL}$. (C) The protein-expression amounts of cell cycle modulators p27, CDK2 and cyclin A, and pro-survival protein XIAP. The results of western blot analysis showed that the micelle/CPT causes a dramatically decreased level of p27 protein in CRL-5802 cells as compared with H1299 cells. β -Actin was used as an internal control for equal loading.

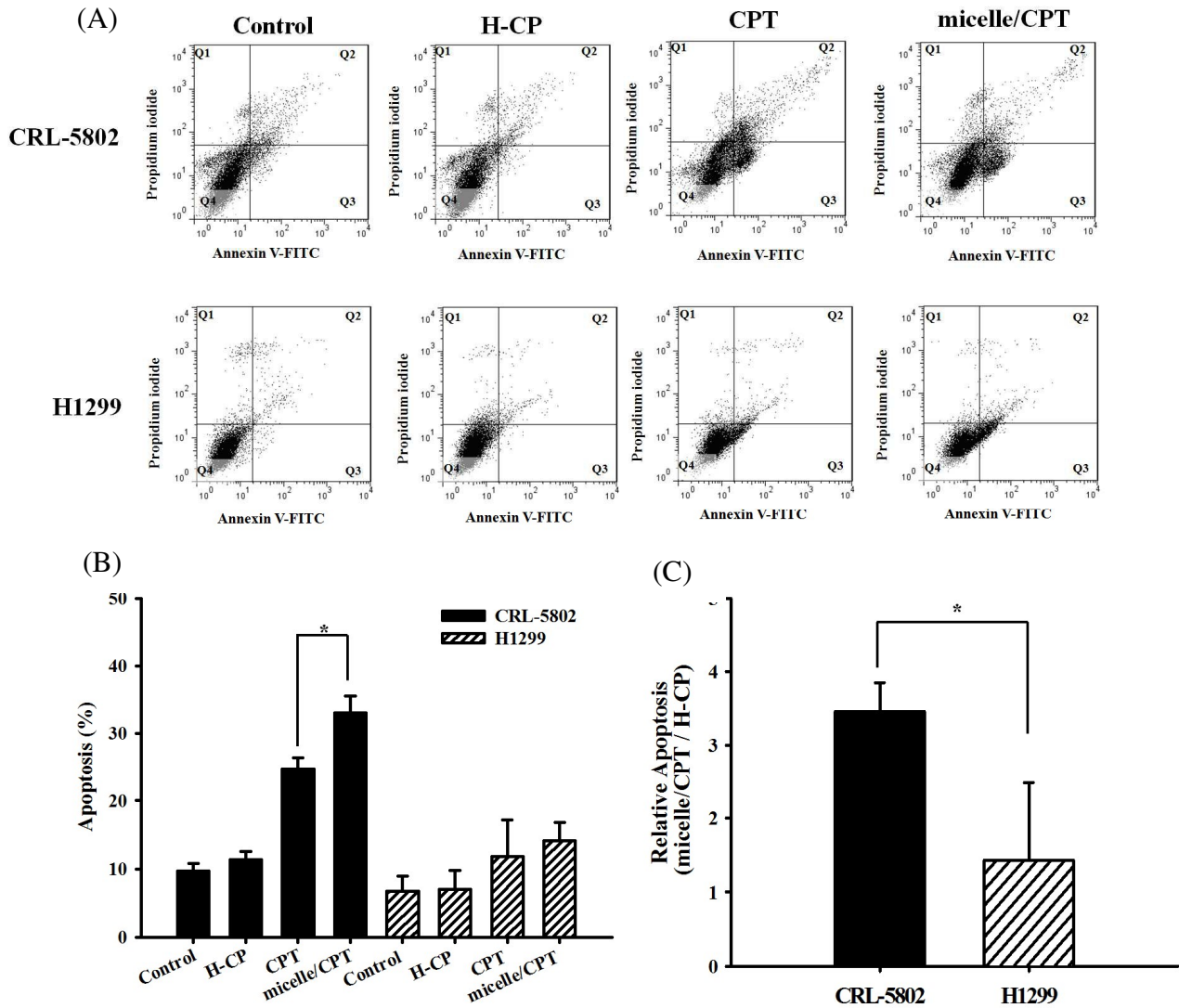
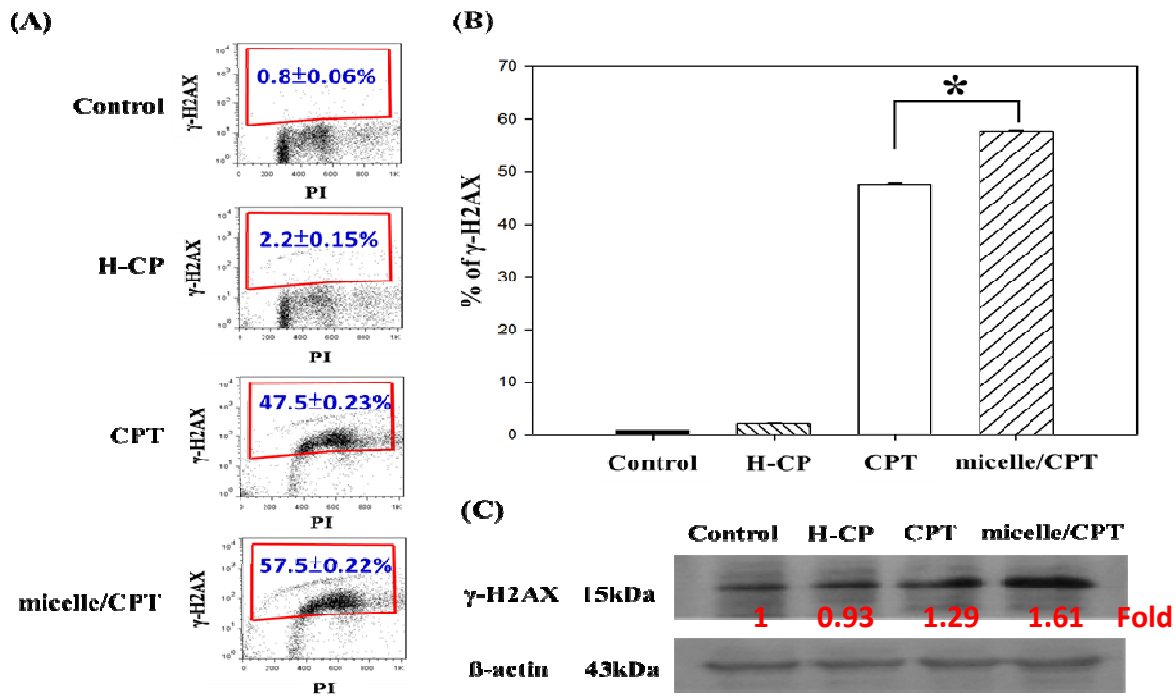


Fig. 5. Induction of apoptosis in CRL-5802 and H1299 cells exposed to H-CP micelle, CPT, and micelle/CPT for 24 hours of incubation at 37 °C using the equivalent CPT concentration of 0.1 μ g/mL. (A) the annexin-V/PI dual staining assay, (B) the percentage of apoptosis cells calculated from (A). (C) The relative apoptosis ratios between cells treated with the micelle/CPT and empty H-CP (n=3, *P< 0.05).

(a) CRL-5802



(b) H1299

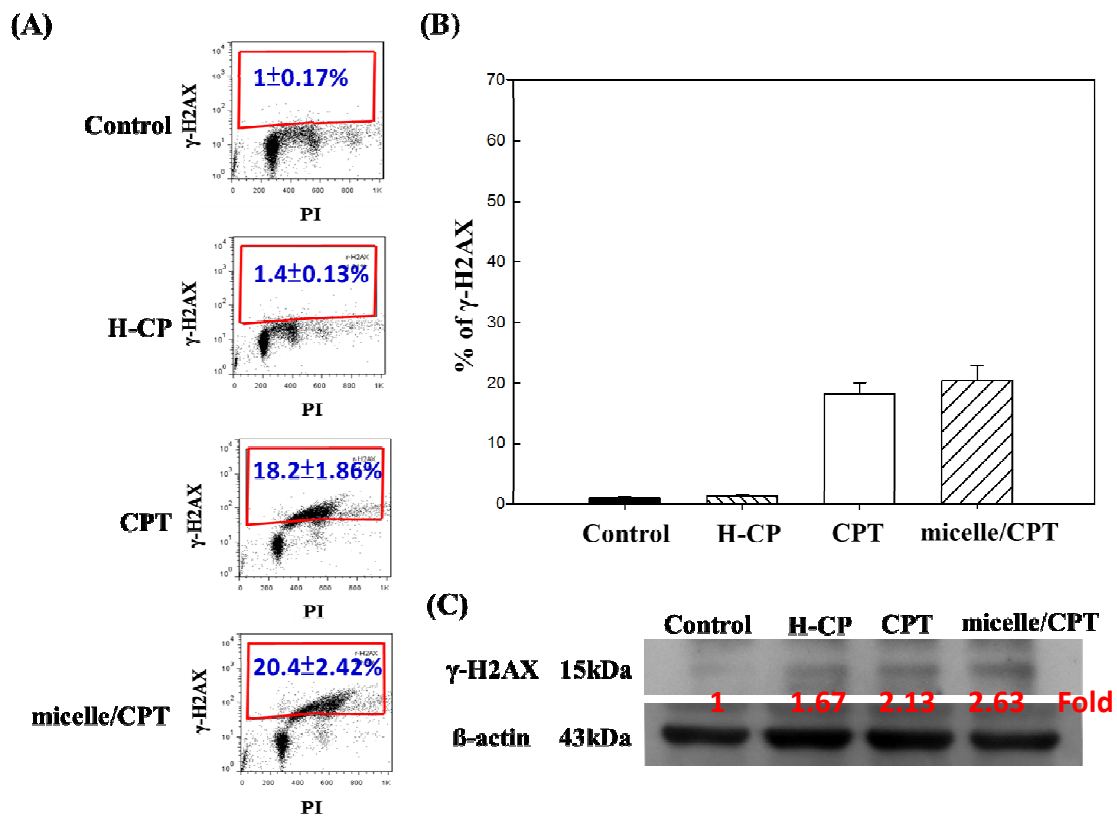


Fig. 6. Formation of γ -H2AX in (a) CRL-5802 cells and (b) H1299 cells exposed to micelle, free CPT, and micelle/CPT for 2 hours of incubation using the equivalent CPT concentration of 0.1 μ g/mL. (A) The expression of γ -H2AX was analyzed by flow cytometry, (B) plotted in percentage of γ -H2AX-positive cells, and (C) done by western blotting analysis (n=3, *P< 0.05). β -Actin was used as an internal control for equal loading.

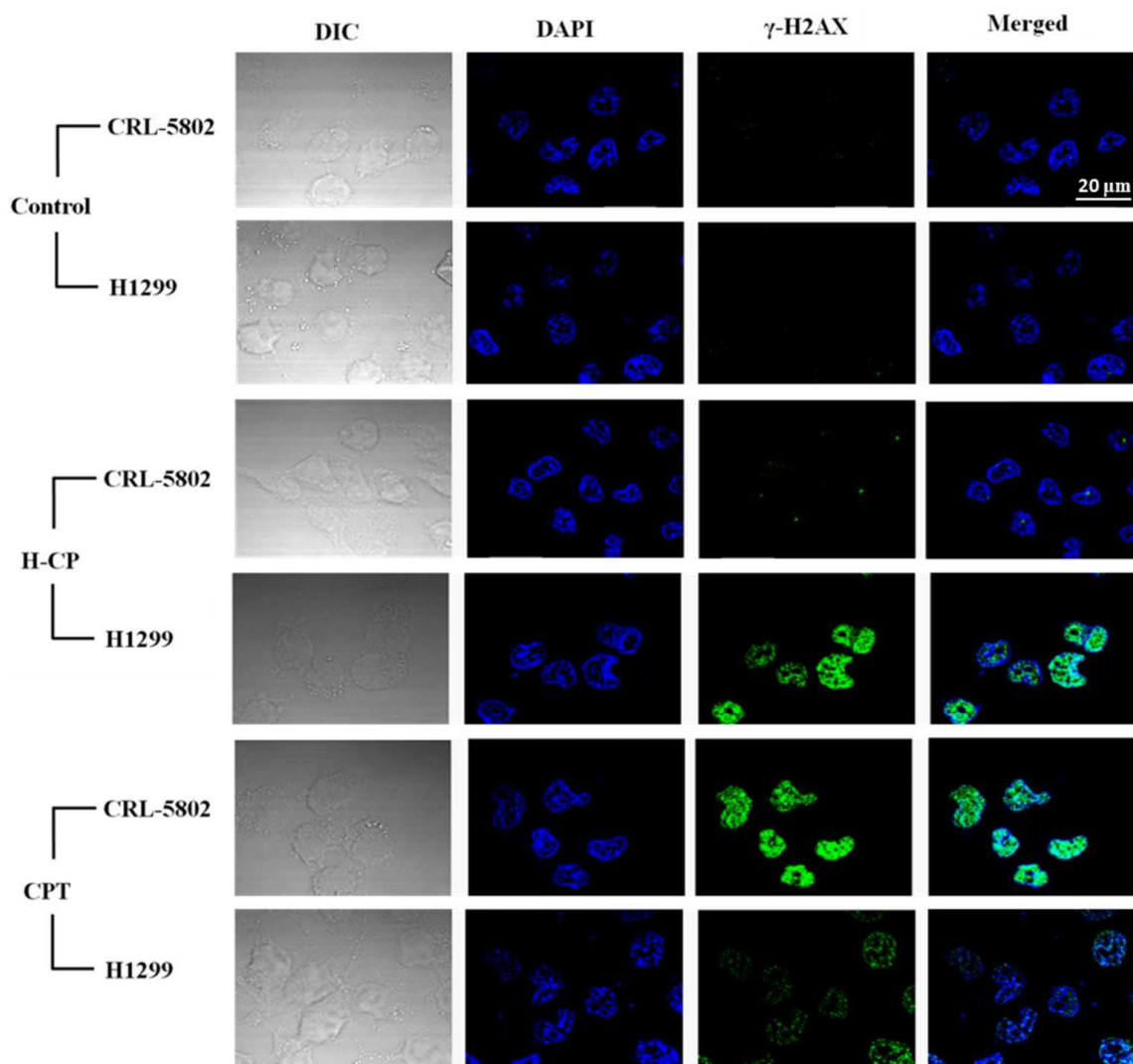
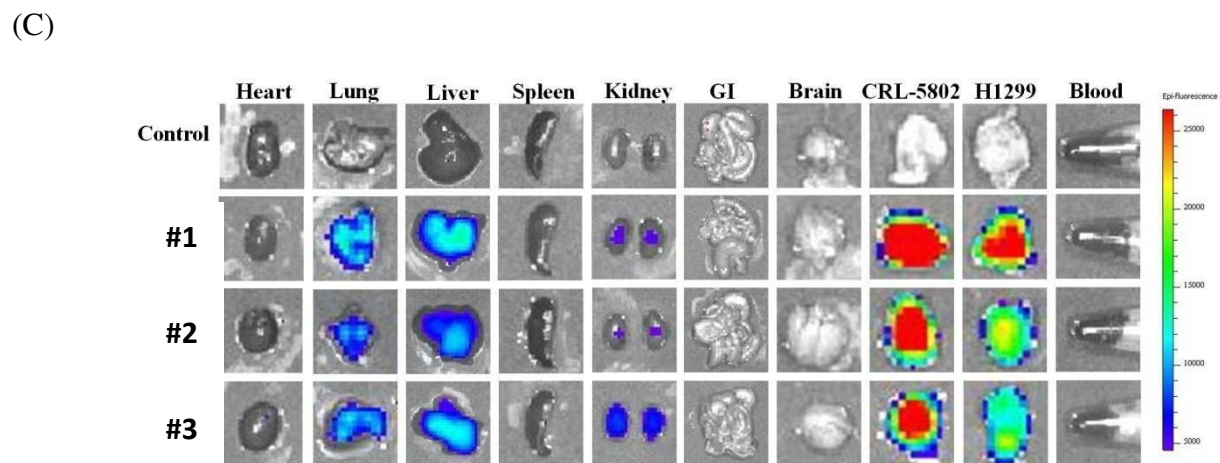
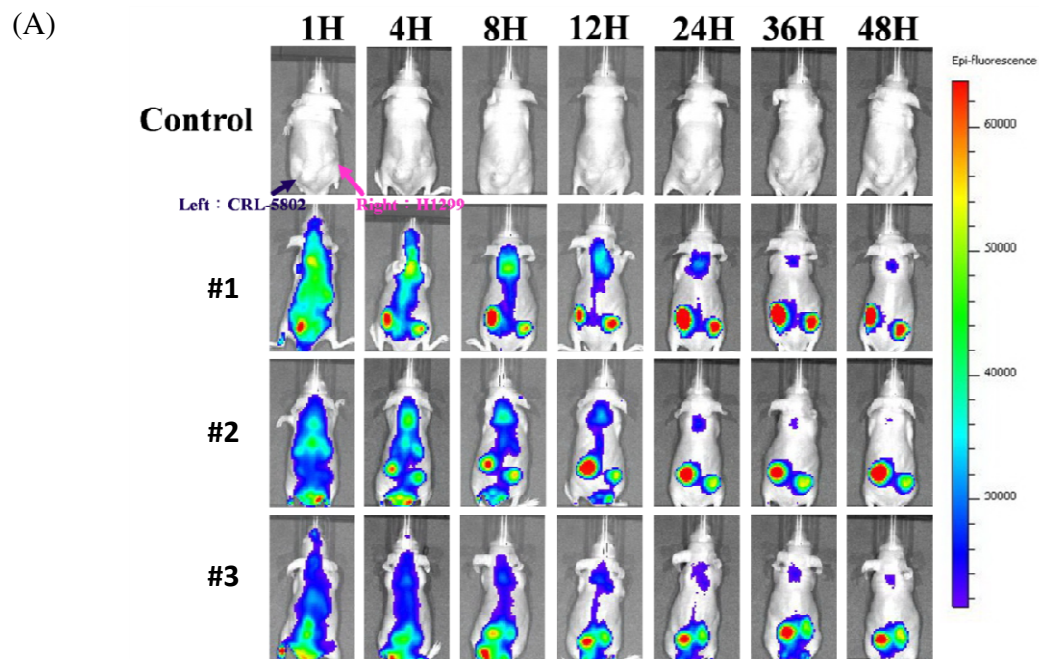
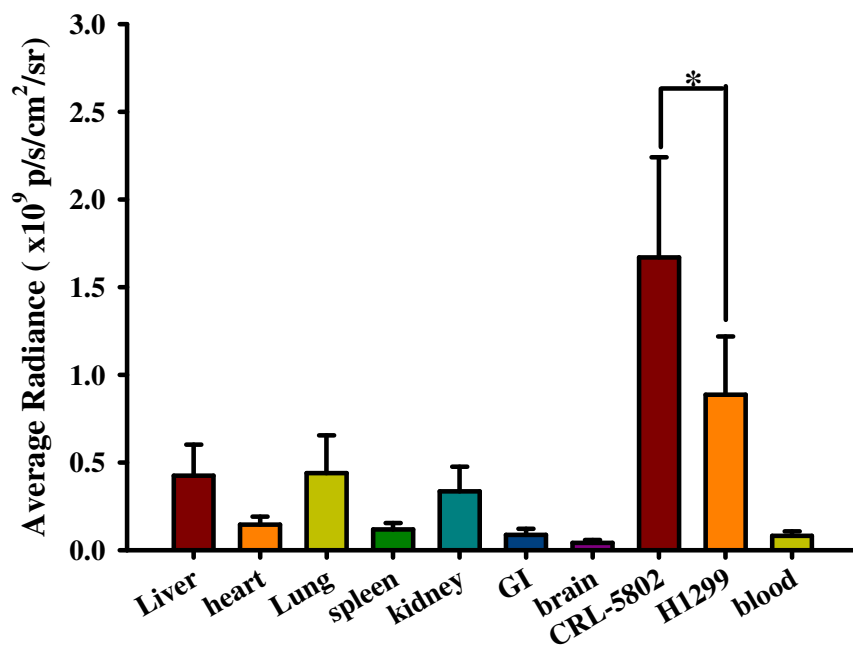


Fig. 7. CLSM images of γ -H2AX in CRL-5802 and H1299 exposed to micelle, free CPT, and micelle/CPT for 2 hours of incubation using the equivalent CPT concentration of 0.1 μ g/mL. The cells nuclei were stained with DAPI in blue and γ -H2AX was stained with p-histone H2AX (Ser 139) monoclonal primary antibody and Alexa Fluor 488-tagged secondary antibody. The formation of γ -H2AX foci was indicated in green fluorescence.



(D)



(E)

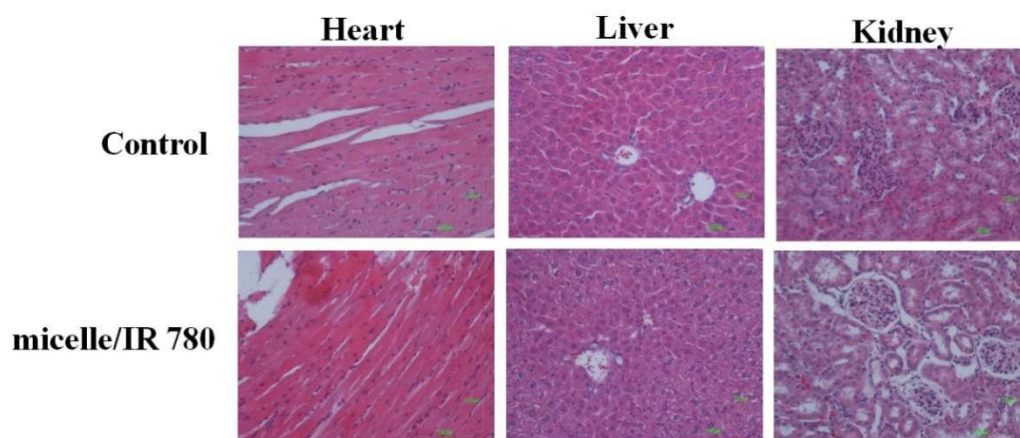


Fig. 8. (A) The optical images of CLR-5802 and H1299 tumors xenografted in male Balb/c mice (~ 6 weeks old, n=3 labeled as #1, 2, 3) using a near-infrared non-invasive optical imaging technique. (B) The tumors isolated to validate similar sizes. (C) The fluorescent images and (D) relative fluorescence intensities of isolated tissues after mice were injected with the IR-780-loaded micelle (micelle/IR 780) for 48 hours. (E) HE analysis of the effect of the micelle on heart, liver, and kidney. (The equivalent concentration of IR780 is 1.75 mg/kg using EX 745 nm and EM 840 nm).